

# Resistor-Network Formulation of Multi-Temperature Free Convection Problems

Sepehr Foroushani\* and John L. Wright†  
*University of Waterloo, Waterloo, ON, N2L 3G1, Canada*

and  
David Naylor‡  
*Ryerson University, Toronto, ON, M5B 2K3, Canada*

**Please note that this file contains the final draft version of this technical paper. Minor differences will be found between this version and the final version printed by the publisher. The reader should contact the publisher if the final version, as printed, is preferred.**

**Copyright © 2016 by the American Institute of Aeronautics and Astronautics, Inc. All rights reserved. Copies of this paper may be made for personal and internal use, on condition that the copier pay the per-copy fee to the Copyright Clearance Center (CCC). All requests for copying and permission to reprint should be submitted to CCC at [www.copyright.com](http://www.copyright.com); employ the ISSN 0887-8722 (print) or 1533-6808 (online) to initiate your request.**

**Foroushani, S., Wright, J. L., & Naylor, D. (2017). Resistor-Network Formulation of Multitemperature Free-Convection Problems. *Journal of Thermophysics and Heat Transfer*, 1–6. <https://doi.org/10.2514/1.T5024>**

---

\* PhD Candidate, Department of Mechanical & Mechatronics Engineering

† Professor, Department of Mechanical & Mechatronics Engineering

‡ Professor, Department of Mechanical & Industrial Engineering

# Resistor-Network Formulation of Multi-Temperature Free Convection Problems

Sepehr Foroushani<sup>§</sup> and John L. Wright<sup>\*\*</sup>  
*University of Waterloo, Waterloo, ON, N2L 3G1, Canada*

and  
David Naylor<sup>††</sup>  
*Ryerson University, Toronto, ON, M5B 2K3, Canada*

In recent work, the resistor-network formulation of forced convection problems and a technique, dQdT, for evaluating the paired convective resistances that characterize the network were presented. This technique entails solutions of the energy equation with perturbed boundary conditions. The resistor-network approach is particularly advantageous for multi-temperature convection problems in that it reveals the split of heat transfer between the different sources. In the present paper, the dQdT technique is extended to free convection. The analytical solution to the classical problem of free convection at an isothermal vertical flat plate is used to verify the technique. Then, dQdT is applied to the three-temperature problem of free convection in an asymmetrically heated vertical channel based on numerical solutions of the energy equation. Sample results are presented and known limits are discussed to demonstrate the validity of the results. This paper is part of a series on the resistor-network formulation of convection problems.

## Nomenclature

$a$	=	constant in Eq. 9
$g$	=	gravitational acceleration [m/s <sup>2</sup> ]
$Gr$	=	Grashof number [-]
$H$	=	plate/channel height [m]

---

<sup>§</sup> PhD Candidate, Department of Mechanical & Mechatronics Engineering

<sup>\*\*</sup> Professor, Department of Mechanical & Mechatronics Engineering

<sup>††</sup> Professor, Department of Mechanical & Industrial Engineering

$k$	=	thermal conductivity [W/mK]
$Nu$	=	local Nusselt number [-]
$\overline{Nu}$	=	average Nusselt number [-]
$Pr$	=	Prandtl number [-]
$Q$	=	heat transfer rate (per unit depth) [W/m]
$q$	=	heat flux [W/m <sup>2</sup> ]
$Ra$	=	Rayleigh number [-]
$R$	=	(unit-depth) thermal resistance [mK/W]
$r_T$	=	temperature ratio [-] (Eq. 21)
$T$	=	temperature [K]
$w$	=	channel width [m]

#### *Greek Symbols*

$\beta$	=	thermal expansion coefficient [1/K]
$\theta$	=	dimensionless temperature [-] (Eq. 23)
$\nu$	=	kinematic viscosity [m <sup>2</sup> /s]
$\Phi$	=	Prandtl number function in Eq. 6 [-]

#### *Subscripts*

$ij$	=	paired: from $i$ to $j$
$0$	=	ambient fluid
$1$	=	left channel wall/ flat plate
$2$	=	right channel wall

#### *Superscripts*

$*$	=	perturbed condition
-----	---	---------------------

## I. Introduction

In many convection problems, heat transfer occurs between two or more isothermal heat sources/sinks. Convective heat transfer in heated passages is a common example. The formulation of this class, multi-temperature convection problems, in terms of a network of convective resistors has several advantages. In recent

work [1,2] the formulation of constant-property multi-temperature forced convection problems in terms of a resistor network was presented. It was shown that the resistor-network approach leads to a simple presentation of the results, eliminates non-physical singularities encountered in the traditional formulation, and, most notably, reveals information not available in the traditional formulation, *i.e.* the split of heat transfer between different sources. The resistor-network approach has been shown to be computationally advantageous in time-step building energy simulations in that it provides detailed heat transfer results at very low computational cost [3,4].

It was further shown [2] that in general it is not possible to find the paired resistances that characterize the resistor network of a multi-temperature convection problem based only on a single analytical or numerical solution, or measurement. Consider, for example, the delta network shown in Figure 1. This network can be used to represent convection in an asymmetrically heated channel where the channel walls are at temperatures  $T_1$  and  $T_2$ , and the fluid flow enters the channel at temperature  $T_0$ .

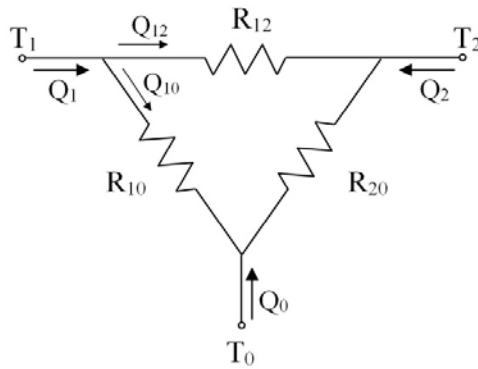


**Figure 1: The delta resistor network of a three-temperature convection problem**

The set of heat transfer rates,  $\{Q_i\}$ , can be obtained for any given set of boundary temperatures,  $\{T_i\}$ . But heat transfer at a node, say  $Q_1$ , is split between the two legs of the network connected to that node. See Equation 1 and Figure 1.

$$Q_1 = Q_{10} + Q_{12} \quad (1)$$

Following the standard electrical analogy for heat transfer, the two “paired” heat transfer component on RHS of Equation 1 can be written in terms of the corresponding driving temperature difference and a paired resistance,  $R_{ij}$ . See Equation 2. The term “paired” emphasizes the idea that  $Q_{ij}$  and  $R_{ij}$  corresponds to a specific pair of nodes,  $T_i$  and  $T_j$ .

$$Q_{ij} = \frac{T_i - T_j}{R_{ij}} \quad (2)$$

Equation 2 gives the definition of  $R_{ij}$ . Three paired convective resistances,  $\{R_{ij}\}$ , characterize the delta network of Figure 1.

Equation 1 can now be recast in terms of the three nodal temperatures, and the paired resistances connected to node 1. See Equation 3.

$$Q_1 = \frac{T_1 - T_0}{R_{10}} + \frac{T_1 - T_2}{R_{12}} \quad (3)$$

Writing an energy balance similar to Equation 3 for the other two nodes, three algebraic equations are obtained with the three resistances,  $\{R_{ij}\}$ , unknown. But these equations are not independent since the overall energy balance of the network requires  $Q_0 + Q_1 + Q_2 = 0$ . The system of equations is under-defined with three unknowns and only two independent equations. It is therefore not possible to determine the paired convective resistances based on the knowledge of the total heat transfer rates only. An additional equation is required.

The dQdT technique was developed [2] to overcome this difficulty and generate additional equations that can be used in conjunction with the nodal energy balances to obtain the paired resistances. This technique entails solutions of the energy equation with perturbed boundary conditions. The dQdT technique [2] gives a paired resistance,  $R_{ij}$ , in a constant-property forced convection problem (where the energy equation is linear) as shown in Equation 4. In this equation,  $\delta T_j$  denotes a perturbation in  $T_j$  and  $\delta Q_i$  denotes the resulting change in  $Q_i$ .

$$R_{ij} = -\frac{\delta T_j}{\delta Q_i} \quad (4)$$

Equation 4 can be implemented analytically or numerically as demonstrated and verified for benchmark forced convection problems [2]. The application of dQdT to turbulent flow is also demonstrated for a forced convection example [2]. In the present work, the resistor-network formulation and the dQdT technique are extended to include variable-property and free-convection cases.

## II. The dQdT Technique Extended

The validity of Equation 4 rests on two key points: constant properties and forced convection, *i.e.* one-way coupling between the velocity and temperature fields. In this case, the energy equation is linear and Equation 4 can be written in differential form, as shown in Equation 5.

$$R_{ij} = \left( -\frac{\partial Q_i}{\partial T_j} \right)^{-1} \quad (5)$$

In general, there may be a two-way coupling between velocity and temperature due to temperature-dependent fluid properties or buoyancy. The accuracy of Equation 5 might hence be undermined.

As an example, consider the classical problem of laminar free convection along an isothermal vertical flat plate. This is a two-temperature problem involving two isothermal sources: the flat plate at  $T_1$  and the far-field ambient at  $T_0$ . The corresponding resistor network entails a single convective resistance,  $R_{10}$ , connecting two temperature nodes,  $T_1$  and  $T_0$ .

The boundary-layer solution by Ostrach [5] gives the average Nusselt number based on the plate height ( $H$ ) in the laminar regime ( $Ra \leq 10^9$ ) as shown in Equation 6. In this equation,  $\Phi$  is a function of the Prandtl number,  $Pr$ , only.

$$\overline{Nu} = \frac{4}{3} \Phi Gr^{\frac{1}{4}} \quad (6)$$

Based on Equation 6, the (per-unit-depth) heat transfer rate at the plate can be calculated as shown in Equation 7.

$$Q_1 = k \overline{Nu} (T_1 - T_2) \quad (7)$$

By definition (Equation 2), the paired resistance  $R_{10}$  will be:

$$R_{10} = \frac{T_1 - T_0}{Q_{10}} = \frac{T_1 - T_0}{Q_1} \quad (8)$$

So for a given fluid, combining Equations 6 to 8, the unit-depth convective resistance,  $R_{10}$ , will be given by Equation 9, where  $\Delta T = T_1 - T_0$  and  $a$  is a constant.

$$R_{10} = \frac{1}{k \overline{Nu}} = a (\Delta T)^{-\frac{1}{4}} \quad (9)$$

To find  $R_{10}$  using Equation 5, on the other hand, Equation 7 must be differentiated:

$$R_{10} = \left( -\frac{\partial Q_1}{\partial T_0} \right)^{-1} = \left( \frac{\partial Q_1}{\partial (\Delta T)} \right)^{-1} = \frac{4}{5} a (\Delta T)^{-\frac{1}{4}} \quad (10)$$

Comparing Equations 9 and 10, it can be seen that  $dQdT$  gives  $R_{10}$  with a bias error of 20%. In general, the relation between  $\{Q_i\}$  and  $\{T_i\}$  is not known in advance. Hence, the bias introduced by applying Equation 2 cannot be estimated and corrected.

To examine the error, the partial derivative in Equation 10 can be written as shown in Equation 11, with  $R_{10}$  and  $\Delta T$  treated separately.

$$-\frac{\partial Q_1}{\partial T_0} = -\frac{\partial}{\partial T_0} \left( \frac{T_1 - T_0}{R_{10}} \right) = \frac{1}{R_{10}} - \left[ \frac{\partial}{\partial T_0} \left( \frac{1}{R_{10}} \right) \right] \Delta T \quad (11)$$

It can be seen that the first term on RHS of Equation 11 gives  $R_{10}$ , the desired value, while the second term produces the 20% bias. To eliminate the error, the second term must be eliminated. This can be achieved by “treating  $R_{10}$  as a constant” when performing the differentiation with respect to  $T_0$ . See Equation 12.

$$-\frac{\partial Q_1}{\partial T_0} \Big|_{R_{10}=\text{const}} = \frac{1}{R_{10}} \quad (12)$$

Hence, in the flat plate example,  $R_{10}$  can be obtained without error as shown in Equation 13.

$$R_{10} = \left( -\frac{\partial Q_1}{\partial T_0} \Big|_{R_{10}=\text{const}} \right)^{-1} = \left( \frac{\partial Q_1}{\partial (\Delta T)} \Big|_{R_{10}=\text{const}} \right)^{-1} = a (\Delta T)^{-\frac{1}{4}} \quad (13)$$

Returning to the more general multi-temperature case, the energy balance at node  $T_i$  requires:

$$Q_i = \sum_j Q_{ij} = \sum_j \frac{T_i - T_j}{R_{ij}} \quad (14)$$

So the change in  $Q_i$  in response to a change in  $T_j$  can be written as shown in Equation 15.

$$\delta Q_i = \left[ \sum_k \frac{\partial}{\partial T_j} \left( \frac{T_i - T_k}{R_{ik}} \right) \right] \delta T_j = \left( -\frac{1}{R_{ij}} + \sum_k \left[ \frac{\partial}{\partial T_j} \left( \frac{1}{R_{ik}} \right) \right] (T_i - T_k) \right) \delta T_j \quad (15)$$

To obtain  $R_{ij}$ ,  $Q_i$  must be linearized with respect to  $\{T_i\}$ , *i.e.* all  $R_{ik}$  must be “held constant.” In this case, the summation on RHS of Equation 15 will be zero and  $R_{ij}$  will be given by Equation 16.

$$R_{ij} = \left( -\frac{\delta Q_i}{\delta T_j} \Big|_{R_{ik}=\text{const}} \right)^{-1} = \left( -\frac{\partial Q_i}{\partial T_j} \Big|_{R_{ik}=\text{const}} \right)^{-1} \quad (16)$$

In constant-property forced convection problems, the  $R_{ik}=\text{const}$  constraint is automatically satisfied due to the one-way coupling between the velocity and temperature fields. For the few free convection problems for which an analytical relation between  $\{Q_i\}$  and  $\{T_i\}$  is at hand, “treating  $R_{ij}$  as constants” can be done by linearizing the expressions for  $\{Q_i\}$  and performing the partial differentiation with respect to  $\{T_i\}$ . In most cases, however, an

analytical solution is not available, but a numerical solution can be obtained. In this situation,  $R_{ik}$  can be held constant numerically using the lemma described in the following section.

### III. Holding $R_{ik}$ Constant: “The Fix”

A convective resistance is known to be a function of geometry, the velocity field and fluid properties. Hence, in a given geometry, the temperature field can influence convective resistances through buoyancy or temperature-dependent fluid properties. In other words, nonlinearities in the energy equation are due to either buoyancy or temperature-dependent properties. Therefore, if the velocity field and fluid properties are “fixed,” *i.e.*, held unchanged, perturbing a temperature will not alter  $\{R_{ik}\}$ . Fixing the fluid properties and the velocity field removes the non-linearities in the energy equation. Recall that the thermal boundary conditions are all linear.

This lemma, linearizing the energy equation by fixing the velocity field and the fluid properties, can be implemented numerically by solving the energy equation with a perturbed boundary condition while retaining the velocity field and fluid properties of the baseline solution (*i.e.* the solution for the original, unperturbed boundary conditions). This will be demonstrated and verified for a classical two-temperature problem as well as a three-temperature example.

### IV. Two-Temperature Example: Laminar free convection at an isothermal vertical flat plate

Consider the classical problem of laminar free convection at an isothermal vertical flat plate. This is a two-temperature problem for which there is no need for  $dQdT$ ; the single convective resistance characterizing the problem can be obtained with an energy balance. See Equation 8. This two-temperature example is used to demonstrate and verify Equation 16: the extended  $dQdT$  technique with  $R_{ik}$  held constant hereinafter called simply  $dQdT$ .

The commercial CFD code ANSYS FLUENT 14.0 [6,7] was used to obtain second-order finite-volume solutions to the mass, momentum and energy equations. The PRESTO! algorithm for discretizing pressure, SIMPLE scheme for handling the pressure-velocity coupling and the Boussinesq approximation for density were used. The corresponding resistor network and a schematic of the computational domain are shown in Figure 2. The boundary conditions used in the CFD solution are listed in the caption of Figure 2.

A baseline numerical solution was obtained and the total heat transfer rate (per unit depth) at the plate,  $Q_1$ , calculated. An average paired Nusselt number, defined by Equation 17, can be used to report results in



dimensionless form. For this two-temperature problem,  $\overline{Nu}_{10}$  can be directly calculated from an energy balance once  $Q_1$  is known. See Equation 17.

$$\overline{Nu}_{10} = \frac{1}{k} \left( \frac{1}{R_{10}} \right) = \frac{1}{k} \left( \frac{Q_{10}}{T_1 - T_0} \right) = \frac{1}{k} \left( \frac{Q_1}{T_1 - T_0} \right) \quad (17)$$

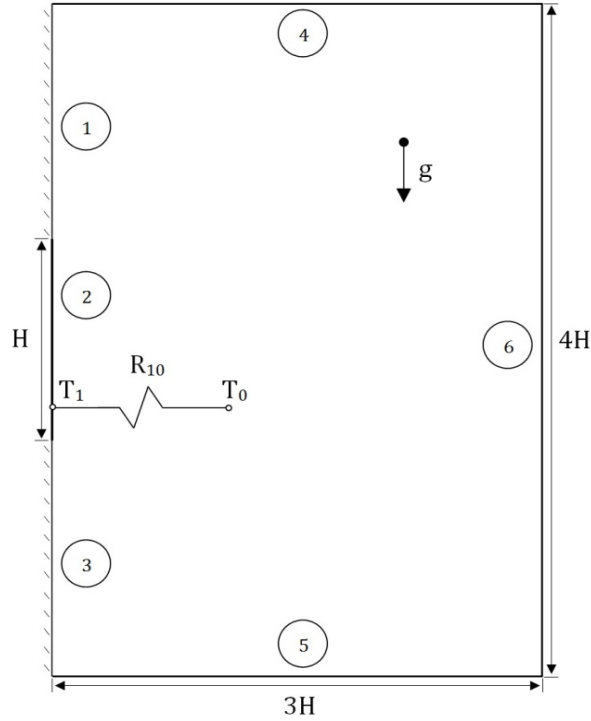


**Figure 2: Free convection at an isothermal vertical flat plate – resistor network and computational domain**

**Boundary conditions: 1,3) adiabatic wall, 2) isothermal wall ( $T_1$ ), 4-6) pressure inlet/outlet ( $p_0, T_0$ )**

In Figure 3, CFD results are compared to the boundary layer solution [5] for  $10^2 < Ra_H < 10^9$ . The approximate curve-fit given in [8] was used to evaluate  $\Phi$  for  $Pr=0.7$ . The agreement between the numerical results and the analytical solution validates the baseline numerical solutions subsequently used for  $dQdT$ .

Next, to apply Equation 16, the ambient temperature,  $T_0$ , was changed by  $\delta T_0$  and a new solution was obtained by updating the temperature field only, while retaining the velocity field of the baseline solution. The new heat transfer rate at the plate,  $Q_1^*$ , and the change  $\delta Q_1 = Q_1^* - Q_1$  were then calculated. The ratio  $\delta Q_1 / \delta T_0$  was then used to calculate  $\overline{Nu}_{10}$ . See Equation 18.

$$\overline{\text{Nu}}_{10} = \frac{1}{k} \left( - \frac{\delta Q_1}{\delta T_0} \Big|_{R_{10}=\text{const}} \right) \quad (18)$$

At  $Ra=10^5$ , for example, with  $H=0.1$  m,  $T_1=310$  K,  $T_0=300$  K, and  $k=0.0255$  W/mK, a total heat transfer rate of  $Q_1=2.3681$  W/m is obtained. Therefore, based on Equation 17:

$$\overline{\text{Nu}}_{10} = \frac{1}{k} \left( \frac{Q_1}{T_1 - T_0} \right) = \frac{1}{0.0255} \left( \frac{2.3681}{310 - 300} \right) = 9.29$$

Then, to apply dQdT,  $T_0$  was changed to  $T_0^*=299$  K and the solution to the energy equation only was updated. In ANSYS FLUENT, this can be easily done by selecting only the energy equation in the “Equations” section, under “Solution Controls.” The new rate of heat transfer at the plate was obtained to be  $Q_1^*=2.6050$  W/m. Hence, based on Equation 18:

$$\overline{\text{Nu}}_{10} = \frac{1}{k} \left( - \frac{\delta Q_1}{\delta T_0} \Big|_{R_{10}=\text{const}} \right) = \frac{1}{0.0255} \left( \frac{2.6050 - 2.3681}{300 - 299} \right) = 9.29$$

In Figure 3, dQdT results are compared to energy balance results (direct CFD, Equation 17) and the boundary layer solution [5]. dQdT results match the CFD results exactly and are in close agreement with the boundary layer solution. Equation 16 is thus verified.

It is noteworthy that since fixing the velocity field and the fluid properties linearizes the energy equation, the size of perturbation,  $\delta T_0$ , does not matter when performing dQdT. Nonetheless, numerical considerations preclude very small perturbations. The perturbation must be large enough that  $\delta Q_1$  can be reliably identified within the numerical accuracy of the solution.

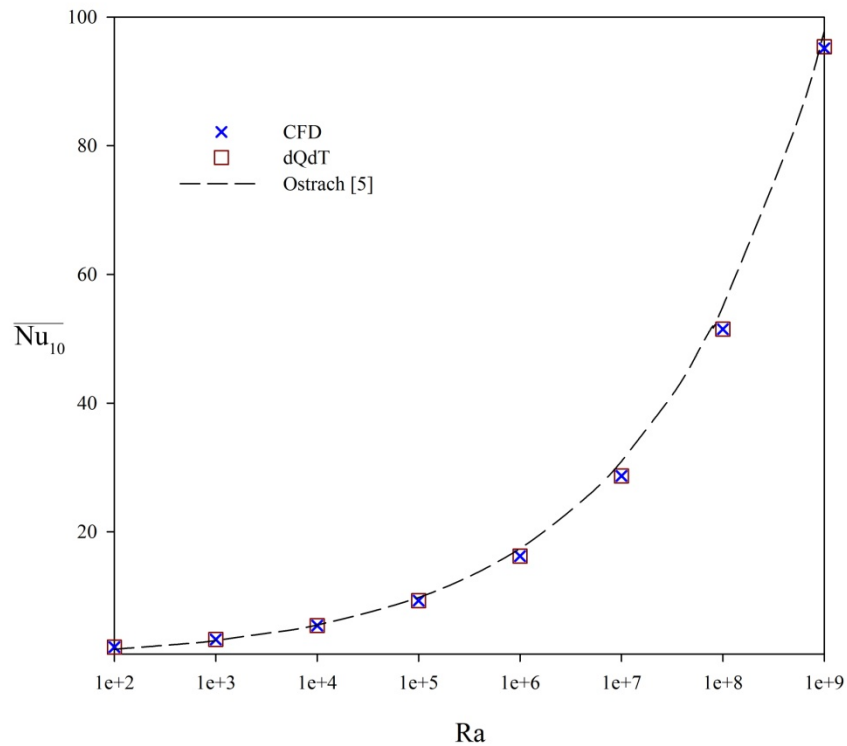


**Figure 3: Average Nusselt number of laminar free convection at a vertical flat plate (Pr=0.7)**

### V. Three-Temperature Example: Laminar free convection in an asymmetrically heated vertical channel

Consider laminar free convection in a tall vertical channel with isothermal walls: a three-temperature problem, shown schematically in Figure 4. The delta network of Figure 1 can be used to represent this configuration. In this network  $T_0$  represents inlet flow, and  $T_1$  and  $T_2$  represent isothermal walls.

To find  $\{\overline{Nu}_{ij}\}$  using dQdT, a second-order finite-volume solution was first obtained using the commercial solver ANSYS FLUENT. The PRESTO! algorithm for discretizing pressure, SIMPLE scheme for handling the pressure-velocity coupling and the Boussinesq approximation for density were used. The boundary conditions are listed in the caption of Figure 4. **To avoid the complexities of simulating turbulent free convection and the various details involved in validating the baseline CFD solutions, and in order to keep the focus on the dQdT technique, only laminar cases were considered.**

A Richardson-extrapolation-based technique [9] was used to assess grid dependence of the solutions. Using three non-uniform rectangular grids with 4400, 27600 and 110000 control volumes, and based on the rate of total heat

transfer to the fluid,  $Q_0$ , a grid convergence index of 3% was calculated. The apparent order of the solution was found to be 2.

Note that as long as the channel is tall enough ( $H/w \geq 10$ ), axial diffusion can be neglected and it can be shown that heat transfer from the channel walls is not a function of the channel aspect ratio. The present numerical results are produced for an aspect ratio of  $H/w=50$ .

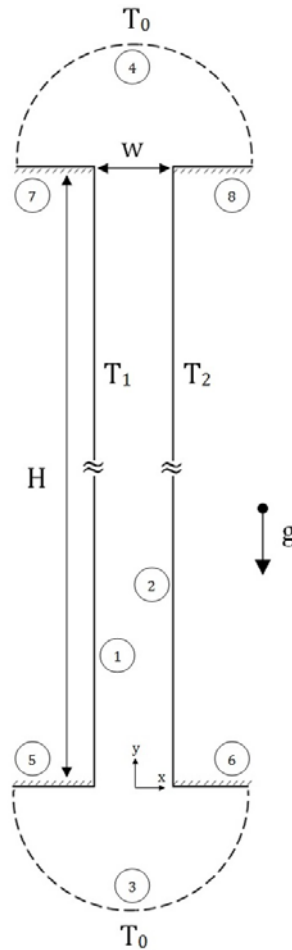


**Figure 4: Computational domain for free convection in an asymmetrically heated vertical channel**  
**Boundary conditions: 1-2) isothermal wall, 3-4) pressure inlet/outlet ( $p_0, T_0$ ), 5-8) adiabatic wall**

To validate the baseline numerical solutions, results were compared to the experimental data of Aung *et al.* [10]. In Figure 5, the local Nusselt number, defined by Equation 19, is shown for  $r_T=0.33$ ,  $Ra=24$  and  $Pr=0.7$ . Definitions of the modified Rayleigh number,  $Ra$ , and the temperature ratio,  $r_T$ , are given in Equations 20 and 21, respectively. In Equation 20,  $T_{wm}$  denotes the mean wall temperature:  $T_{wm} = (T_1 + T_2)/2$ .

$$\text{Nu}_i = \frac{q_i}{(T_1 - T_0)} \left( \frac{w}{k} \right) \quad (19)$$

$$\text{Ra} = \frac{g\beta(T_{wm} - T_0)w^3}{\nu^2} \text{Pr} \left( \frac{w}{H} \right) \quad (20)$$

$$r_T = \frac{T_2 - T_0}{T_1 - T_0} \quad (21)$$

Away from the channel inlet ( $y/H \geq 0.1$ ), the present numerical results are in very close agreement with the measurements. Aung *et al.* [10] reported a drop in the channel wall temperature near the inlet “due to the construction of the apparatus.” This experimental error explains the pronounced discrepancy between numerical and experimental results near the inlet.

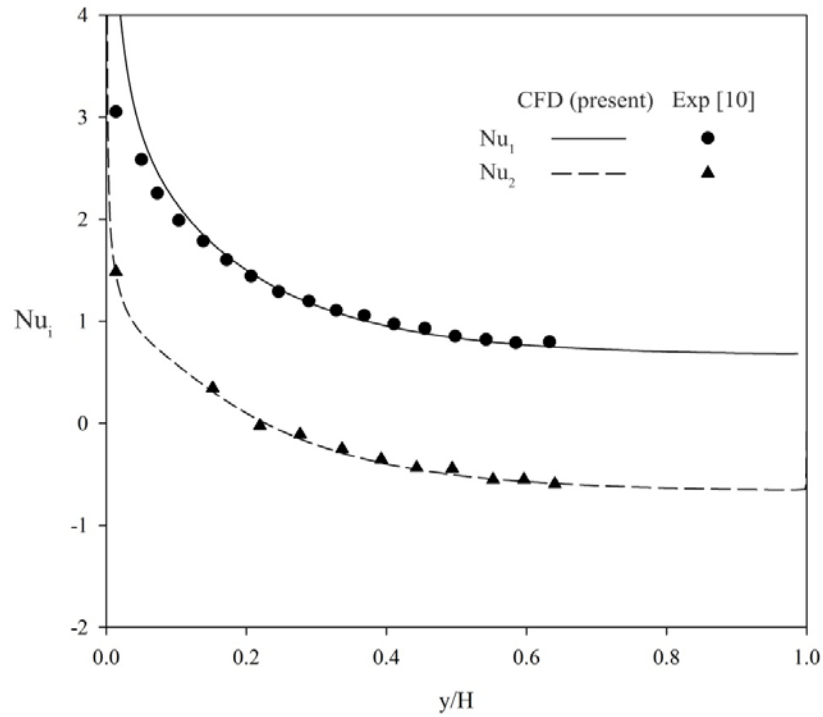


**Figure 5: Local Nusselt numbers in laminar free convection in an asymmetrically heated vertical channel (Ra=24, Pr=0.7, r<sub>T</sub>=0.33)**

At a higher Rayleigh number, Ra=2000, and with the walls symmetrically heated ( $r_T=1$ ), the current CFD solution predicts an average Nusselt number of  $\overline{\text{Nu}}_1 = \overline{\text{Nu}}_2 = 3.93$  which is within 8% of the measured value of 4.27, reported in reference [10].

In the previous section, the validity of Equation 16 was demonstrated for a benchmark two-temperature case. The special case of symmetric heating,  $r_T=1$ , can be used to verify dQdT for this three-temperature problem. When the channel walls are at the same temperature, the velocity field (as well as the fluid properties) are symmetric with respect to the channel centreline ( $x=0$ ). In this case, similar to the forced convection problem studied in [1], the two wall-to-fluid convective resistances are equal, reducing the number of the unknowns to two. The wall-to-fluid resistance,  $R_{10}=R_{20}$ , can then be calculated from the nodal energy balance at either  $T_1$  or  $T_2$  [1]:

$$R_{10} = R_{20} = \frac{T_1 + T_2 - 2T_0}{Q_1 + Q_2} \quad (22)$$

In Table 1 numerical results are presented for a sample symmetric case ( $r_T=1$ ) with  $Ra=24$  and  $Pr=0.7$ , in terms of dimensionless temperature,  $\theta$ , and average Nusselt number (dimensionless heat transfer rate),  $\overline{Nu}$  :

$$\theta_i = \frac{T_i - T_0}{T_1 - T_0} \quad (23)$$

$$\overline{Nu}_i = \frac{Q_i}{kH \left( \frac{T_1 - T_0}{w} \right)} \quad (24)$$

To report paired heat transfer rates,  $Q_{ij}$ , in dimensionless form, an average paired Nusselt number is defined as shown in Equation 25.

$$\overline{Nu}_{ij} = \left( \frac{Q_{ij}/A_i}{T_i - T_j} \right) \frac{w}{k} = \left( \frac{1}{R_{ij}} \right) \frac{w}{kH} \quad (25)$$

Using Equation 22 and the results shown in Table 1, the average wall-to-fluid Nusselt number can be obtained:

$$\overline{Nu}_{10} = \left( \frac{1}{R_{10}} \right) \frac{w}{kH} = \frac{\overline{Nu}_1 + \overline{Nu}_2}{\theta_1 + \theta_2 - 2\theta_0} = \overline{Nu}_1 = 0.073 \quad (26)$$

Also in Table 1,  $\{\overline{Nu}_i^*\}$ , calculated by perturbing  $T_0$  and updating the temperature field while retaining the velocity and density fields of the baseline solution, is reported. Applying dQdT,  $\overline{Nu}_{10}$  is found to be:

$$\overline{Nu}_{10} = \left( \frac{1}{R_{10}} \right) \frac{w}{kH} = \left( - \frac{\delta Q_1}{\delta T_0} \Big|_{R_{ik}=\text{const}} \right) \frac{w}{kH} = - \frac{\delta \overline{Nu}_1}{\delta \theta_0} = 0.073 \quad (27)$$

The results of Equations 26 and 27 are in good agreement, verifying the dQdT technique (Equation 16).

Note that since  $T_1-T_2=0$ ,  $\overline{Nu}_{12}$  cannot be found from nodal energy balances, but it can be obtained using dQdT.

Further note that  $\overline{Nu}_{10}$  and  $\overline{Nu}_{20}$  calculated separately using dQdT confirm  $\overline{Nu}_{10} = \overline{Nu}_{20}$ .

With the baseline CFD solutions validated, dQdT was applied to asymmetric cases with  $r_T=0.5$  and different flow rates,  $0.01 < Ra < 2000$ . Results are shown in Figure 6. For low flow rates,  $Ra < 1$ , heat transfer is dominated by conduction between the walls, leading to  $\overline{Nu}_{12} = 1$ . In this region, there is almost no heat transfer to the fluid:  $\overline{Nu}_{10} \approx \overline{Nu}_{20} \approx 0$ . As the flow rate increases, wall-to-fluid heat transfer is enhanced while wall-to-wall heat transfer decreases. Note that since  $T_1 > T_2$ ,  $\overline{Nu}_{10} > \overline{Nu}_{20}$ . The difference between  $\overline{Nu}_{10}$  and  $\overline{Nu}_{20}$  increases with Ra.

**Table 1: Baseline and perturbed heat transfer rates for laminar free convection in a symmetrically heated vertical channel (Ra=24, Pr=0.7,  $r_T=1$ )**

i	$\theta_i$	$\overline{Nu}_i$	$\theta_i^*$	$\delta\theta_i^*$	$\overline{Nu}_i^*$	$\delta\overline{Nu}_i$
0	0.0	-0.1454	0.1	0.1	-0.1309	0.0145
1	1.0	0.0727	1.0	0.0	0.0654	-0.0073
2	1.0	0.0727	1.0	0.0	0.0654	-0.0073

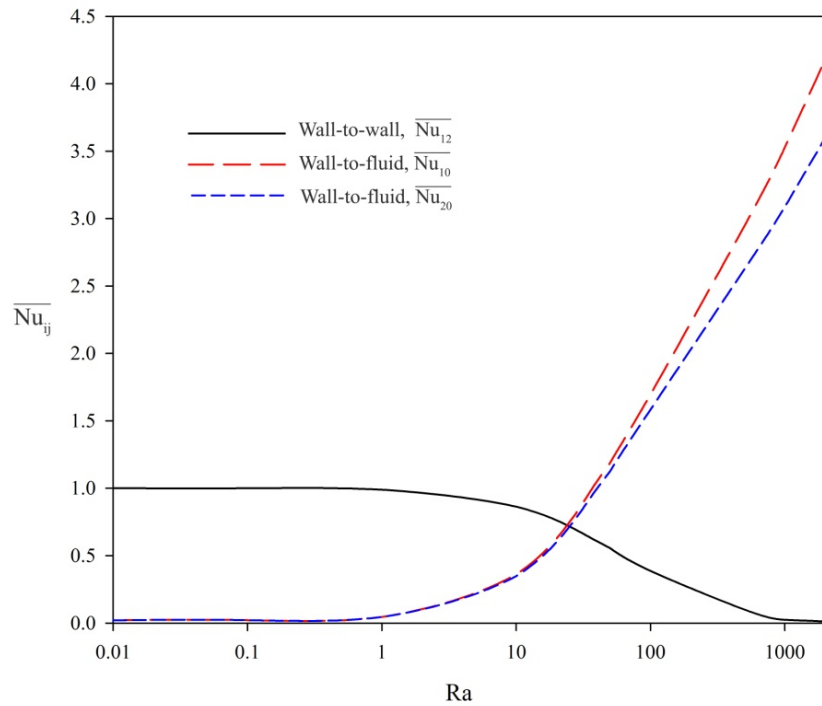


**Figure 6: Average paired Nusselt numbers of laminar free convection in an asymmetrically heated vertical channel ( $r_T=0.5$ , Pr=0.7) obtained using dQdT**

With the channel aspect ratio incorporated into the definition of the “modified” channel Rayleigh number (Equation 20),  $Ra$  is also an indication of the thermal development length. So,  $Ra < 1$  corresponds to the thermally developed limit well downstream in tall channel ( $y \gg w$ ) where heat transfer occurs only between the channel walls with  $\overline{Nu}_{12} = 1$ . The limit where  $Ra \gg 1$ , on the other hand, represents the entrance region of the channel where there is significant wall-to-fluid heat transfer but no wall-to-wall heat transfer.

The validity of the dQdT results for the asymmetric, three-temperature case can be demonstrated by further examining the  $Ra \gg 1$  limit. In this limit, the thermal boundary layers are separated by a core of fluid flow at  $T_0$  and do not thermally communicate. Therefore,  $Q_{12} = 0$ . Wall-to-fluid heat transfer can hence be found by evaluating the total heat transfer at the walls. Focusing on the wall at  $T_1$ , for example:

$$Q_{10} = Q_1 = \int_0^H -k \frac{\partial T}{\partial x} dy \quad ; \quad Ra \gg 1 \quad (28)$$

Heat transfer between either wall and the fluid can also be calculated by evaluating the enthalpy change inside the respective boundary layer. See Equation 29 where  $\delta_1$  is the thickness of the thermal boundary layer developed along the wall at  $T_1$ , and  $v$  is the velocity in the  $y$  direction.

$$Q_{10} = \int_{-\frac{w}{2}}^{\delta_1} \rho v c_p (T - T_0) dx \quad ; \quad Ra \gg 1 \quad (29)$$

The above estimates for  $Q_{10}$  can then be used to evaluate  $\overline{Nu}_{10}$  based on Equation 25. For  $r_T = 0.5$ ,  $Ra = 2000$  and  $Pr = 0.7$ , for example, dQdT gives  $\overline{Nu}_{10} = 4.18$ , while Equations 28 (wall energy balance) and 29 (boundary-layer energy balance, BL) yield  $\overline{Nu}_{10} = 4.18$  and  $\overline{Nu}_{10} = 4.24$ , respectively. Again, the close agreement between the results verifies dQdT.

## VI. Conclusion

The formulation of multi-temperature convection problems in terms of network of convective resistors has been shown to be advantageous. The dQdT technique, which entails solutions of the energy equation with perturbed boundary conditions, gives the paired resistances that characterize such a network. In the present paper, the dQdT technique was extended to the general problem of multi-temperature convection, particularly free convection. In general the flow-field may depend on the temperature field through temperature-dependent properties or buoyancy. Accordingly, the perturbation procedure, which is the basis of the dQdT technique, needs to be modified. It was



demonstrated that the key to implementing dQdT in this case is solving the energy equation with a perturbed boundary condition while retaining the velocity field and fluid properties of the baseline solution.

The boundary-layer solution to the classical problem of free convection at an isothermal vertical flat plate was used to verify the extended dQdT technique. dQdT was also applied to find the paired resistances of a three-temperature problem: **laminar free convection** in an asymmetrically heated vertical channel. Results were verified against energy-balance results for the special case of symmetric heating. The dQdT technique was then applied to generate sample results for asymmetric cases. The validity of the results was further demonstrated by examining known limits. The application of dQdT to turbulent forced convection problem has been presented in previous work.

**Turbulent free convection will be the subject of future work.**

This work is part of an ongoing project on the modeling and characterization of multi-temperature convection problems in terms of resistor networks. The motivation behind this project is modeling heat transfer at windows with shading attachments for building energy simulation applications. With the resistor-network formulation and the dQdT technique extended to free convection, future work will present the applications of this approach, particularly to free convection in asymmetrically heated channels under different temperature arrangements and flow regimes.

### **Acknowledgments**

The financial support of the Smart Net-Zero Energy Buildings Strategic Research Network (SNEBRN) of the Natural Sciences and Engineering Research Council of Canada (NSERC) and the University of Waterloo is hereby acknowledged.

### **References**

- [1] Foroushani, S., Wright, J.L. and Naylor, D., "Asymmetric Graetz Problem: The Analytical Solution Revisited," *AIAA J. Thermophysics & Heat Transfer*, 2016.  
**DOI: 10.2514/1.T4944**
- [2] Foroushani, S., Naylor, D. and Wright, J.L., "Resistor-Network Formulation of Multitemperature Forced-Convection Problems," *AIAA J. Thermophysics & Heat Transfer*, 2016.  
**DOI: 10.2514/1.T4993**
- [3] Wright, J. L., Barnaby, C. S., Niles, P., and Rogalsky, C. J., "Efficient Simulation of Complex Fenestration Systems in Heat Balance Room Models," 12th International Conference of the International Building Performance Simulation Association, International Building Performance Simulation Assoc. (IBPSA), Sydney, Australia, 2011, pp. 2851–2858.

- [4] Barnaby, C.S., Wright, J.L., and Collins, M.R., "Improving Load Calculations for Fenestration with Shading Devices," *ASHRAE Transactions*, Vol. 115, Part 2, 2009, pp. 31, 44.
- [5] Ostrach, S., "An Analysis of Laminar Free-Convection Flow and Heat Transfer about a Flat Plate Parallel to the Direction of the Generating Body Force," NACA Technical Report 1111, 1953.
- [6] ANSYS, 2011, "ANSYS FLUENT User's Guide," ANSYS, Inc., Canonsburg, PA.
- [7] ANSYS, 2011, "ANSYS FLUENT Theory Guide," ANSYS, Inc., Canonsburg, PA.
- [8] Oosthuizen, P. H., and Naylor, D. 1999. *Convective Heat Transfer Analysis*, WCB/McGraw- Hill, New York, Chap. 6.
- [9] Celik, I.B., Ghia, U., Roache, P.J., Freita, C.J., Coleman, H., and Raad, P.E., "Procedure for estimation and reporting of uncertainty due to discretization in CFD Applications," *J. Fluids Eng.*, vol. 130, 2008, pp. 0780011-0780014.  
DOI: 10.1115/1.2960953
- [10] Aung, W., Fletcher, L. S., and Sernas, V., "Developing Laminar Free Convection between Vertical Flat Plates with Asymmetric Heating," *Int. J. Heat Mass Transfer*, vol. 15, 1972, pp. 2293–2308.  
DOI: 10.1016/0017-9310(72)90048-8